JOURNAL OF GENERAL VIROLOGY

RESEARCH ARTICLE

Duncan *et al.*, *Journal of General Virology* 2025;106:002120
DOI 10.1099/jgv.0.002120

MICROBIOLOGY SOCIETY

OPEN ACCESS

# *Wisteria floribunda* agglutinin enhances *Zaire ebolavirus* entry through interactions at specific *N*-linked glycosylation sites on the virus glycoprotein complex

Joshua D. Duncan[1,2,3], Monika Pathak[1,2,4], Barnabas J. King[1,2], Holly Bamber[1,2], Paul Radford[1,2], Jayasree Dey[1,2], Charlotte Richardson[1], Stuart Astbury[5,6], Patrick McClure[1,2,5], Jonathan K. Ball[1,2,5,7], Richard A. Urbanowicz[8,†] and Alexander W. Tarr[1,2,5,*,†]

**Abstract**

Entry of *Zaire ebolavirus* (EBOV) into a host cell is a complex process requiring interactions between the viral glycoproteins (GPs) and cellular factors. These entry factors are cell-specific and can include cell surface lectins and phosphatidylserine receptors. Niemann–Pick type C1 is critical to the late stage of the entry process. Entry has been demonstrated to be enhanced by interactions between the virion and surface-expressed lectins, which interact with carbohydrate moieties attached to the GP. In addition, soluble lectins, including mannose-binding lectin, can enhance entry *in vitro*. However, the mechanism of lectin-mediated enhancement remains to be defined. This study investigated the possibility that plant lectins, *Wisteria floribunda* agglutinin (WFA), soybean agglutinin (SBA) and *Galanthus nivalis* agglutinin (GNA), which possess different carbohydrate-binding specificities, influence EBOV entry. WFA was observed to potently enhance entry of lentiviral pseudotype viruses (PVs) expressing the GP of three *Ebolavirus* species [Zaire, Sudan (*Sudan ebolavirus*) and Reston (*Reston ebolavirus*)], with the greatest impact on EBOV. SBA had a modest enhancing effect on entry that was specific to EBOV, whilst GNA had no impact on the entry of any of the *Ebolavirus* species. None of the lectins enhanced the entry of control PVs expressing the surface proteins of other RNA viruses tested. WFA was demonstrated to bind directly with the EBOV-GP via the glycans, and mutational analysis implicated $N^{238}$ as contributing to the interaction. Furthermore, enhancement was observed in both human and bat cell lines, indicating a highly conserved mechanism of action. We conclude that the binding of WFA to EBOV-GP through interactions including the glycan at $N^{238}$ results in GP alterations that enhance entry, providing evidence of a mechanism for lectin-mediated virus entry enhancement. Targeting lectin-ligand interactions presents a potential strategy for restricting *Ebolavirus* entry.

## DATA AVAILABILITY

The EBOV-GP amino acid sequence used in this study was retrieved from UniProt (accession number Q05320). Protein structures used for modelling are available from the RCSB Protein Data Bank (EBOV-GP 6VKM, mAb KZ52 3CSY and WFA 5KXB).

Received 18 December 2024; Accepted 21 May 2025; Published 06 June 2025
**Author affiliations:** [1]School of Life Sciences, Faculty of Medicine and Health Sciences, The University of Nottingham, Nottingham, UK; [2]Wolfson Centre for Global Virus Research, The University of Nottingham, Nottingham, UK; [3]School of Chemistry, The University of Nottingham, Nottingham, NG7 2RD, UK; [4]School of Pharmacy, Biodiscovery Institute, The University of Nottingham, Nottingham, UK; [5]NIHR Biomedical Research Centre, Nottingham University Hospitals NHS Trust, Nottingham, UK; [6]Nottingham Digestive Diseases Centre, School of Medicine, University of Nottingham, Nottingham, UK; [7]Department of Tropical Disease Biology, Liverpool School of Tropical Medicine, Liverpool, L3 5QA, UK; [8]Department of Infection Biology and Microbiomes, Institute of Infection, Veterinary and Ecological Sciences, The University of Liverpool, Liverpool, UK.
***Correspondence:** Alexander W. Tarr, alex.tarr@nottingham.ac.uk
**Keywords:** Ebola virus; enhancement; lectin; pseudotype; virus entry.
**Abbreviations:** DC-SIGN, dendritic cell-specific ICAM3-grabbing non-integrin; EBOV, *Zaire ebolavirus*; GNA, *Galanthus nivalis* agglutinin; GPs, glycoproteins; HCV, hepatitis C virus; hMGL, human macrophage lectin specific for galactose/*N*-acetylgalactosamine; LCMV, *lymphocytic choriomeningitis mammarenavirus*; LSECtin, liver and lymph node sinusoidal endothelial cell C-type lectin; L-SIGN, liver/lymph node-specific ICAM3-grabbing non-integrin; MBL, mannose-binding lectin; MLD, mucin-like domain; NPC1, Niemann–Pick type C1; PEI, polyethylenimine; PVs, pseudotype viruses; RABV, *Rabies lyssavirus*; RESTV, *Reston ebolavirus*; SBA, soybean agglutinin; SUDV, *Sudan ebolavirus*; VSV, *Indiana vesiculovirus*; WFA, *Wisteria floribunda* agglutinin.
†These authors contributed equally to this work
Six supplementary figures and two supplementary tables are available with the online version of this article.

## INTRODUCTION

*Zaire ebolavirus* (EBOV) is a negative-strand RNA virus that represents a significant threat to human health. EBOV infection causes haemorrhagic fever [1], resulting in a case fatality rate of 60–90% [2]. Since its discovery in 1976, EBOV has been associated with multiple outbreaks in central Africa, the largest of which being the 2018–2020 North Kivu epidemic in the Democratic Republic of the Congo, and the 2013–2016 epidemic in West Africa which resulted in 2,200 and 11,000 deaths, respectively [3, 4]. These outbreaks are believed to result from spillover events originating from an as-yet unidentified animal reservoir(s).

EBOV encodes an envelope glycoprotein (GP) complex that is incorporated onto the surface of the filamentous virion. GP comprises covalently linked heterodimers of $GP_1$ and $GP_2$ subunits and acts as a class I fusion protein, mediating host cell entry via cellular attachment and membrane fusion within late-stage endosomes [5–7]. The N-terminus possesses the $GP_1$ subunit, which possesses a glycan cap that masks the $GP_2$ subunit that contains the fusion peptide [7, 8]. EBOV entry requires cleavage of the GP in the endosome to remove the glycan cap [9], exposing the binding site for the cholesterol transporter protein, Niemann–Pick type C1 (NPC1) [10, 11]. This binding site is located in a pocket in the $GP_1$ molecule, involving amino acids $T^{83}$, $I^{113}$ and $L^{122}$ [11].

During maturation, the EBOV-GP undergoes extensive modification via *N*-, *O*- and *C*-linked glycosylation, leading to the occlusion of epitopes from recognition by host antibodies [12] and receptor attachment [13]. Removal of the carbohydrate from the GP complex is an essential step in entry. A total of 17 predicted *N*-linked glycosylation sites exist in Zaire EBOV-GP, 15 of which are in the $GP_1$ subunit and predominantly located within the glycan cap and mucin-like domain (MLD) regions. Glycan profiling has shown that when expressed in human cells, these sites are occupied by simple mannose or complex oligosaccharides, indicating that processing of the EBOV-GP occurs in the Golgi apparatus [13]. The glycosylation of GP is complex, with varying sugars present at specific *N*-linked sites, and substantial *O*-linked glycosylation occurring in the MLD [13]. One site in the glycan cap ($N^{257}$) has been found to have a restricted, mannose-type sugar, in contrast to the complex glycosylation exhibited at other sites [13].

The extensive glycosylation of the GP facilitates EBOV entry [14]. Interaction with lectins has been proposed as potential attachment receptors [15], but evidence of their role as definitive entry receptors is lacking [16]. Lectins are a diverse group of proteins that possess a range of different carbohydrate-binding specificities. In humans, they contribute to innate immunity by sensing pathogen-associated molecular patterns [17, 18]. Interactions between lectins and viruses can have differing consequences. Soluble lectins can effectively neutralize virus particles through direct interactions with virus GPs [19–24]. Conversely, transmembrane lectins, such as human macrophage C-type lectin and dendritic cell- or liver/lymph node-specific ICAM3-grabbing non-integrin (DC-SIGN; CD209), CLEC4M/L-SIGN (CD299), human macrophage lectin specific for galactose/*N*-acetylgalactosamine (hMGL), liver and lymph node sinusoidal endothelial cell C-type lectin (LSECtin) and asialoglycoprotein receptor I all enhance *in vitro* EBOV entry in specific cell types [25, 26]. However, the C-type lectins are not essential for entry, as evidenced by their negligible expression on some permissive cell types [27], and their inability to confer susceptibility to non-permissive cells [16, 28].

In addition to membrane-associated lectins, secreted lectins such as mannose-binding lectin (MBL) have been demonstrated to enhance infection. MBL is a soluble component of the humoral innate immune response. Through recognition of pathogen-associated carbohydrate patterns, MBL can opsonize a target leading to neutralization. MBL has previously been shown to neutralize a variety of viruses [18]. In the context of EBOV, MBL exhibits complement-dependent neutralizing activity towards retroviral pseudotyped particles bearing authentic EBOV-GP [29] and can protect against lethal challenge [30]. Strikingly, however, in the absence of complement, MBL enhances EBOV cellular entry [31]. This enhancement has been proposed to be a function of MBL directly coupling virus particles to cell surfaces, acting as a 'bridging' receptor and promoting uptake into endosomes [31, 32].

Plant-derived lectins, in addition to those expressed by animal cells, have been studied for their antiviral activity and their use in characterizing the glycan profiles of viral GPs through large lectin-based arrays [33]. Antiviral activity of plant lectins towards a wide range of viruses has been reported [34]. The mechanisms of antiviral activity by lectins vary, with some blocking viral replication and others neutralizing virus entry into a host cell [35]. For example, BanLec, a lectin derived from *Musa acuminata* [36], has previously been shown to inhibit both EBOV replication and entry [37]. As such, plant lectins have potential as inhibitors for virus infections. A broad-spectrum antiviral protein may have application in the public health response to emerging virus infections.

In this study, we addressed the possibility that interactions between soluble lectins with EBOV-GP enhance infection without the requirement for a proposed cell-expressed lectin-binding receptor. The ability of plant-derived lectins with different carbohydrate-binding specificities to enhance EBOV-GP-mediated transduction of permissive cells was assessed. Using a retroviral pseudotype entry model incorporating full-length authentic EBOV-GP proteins [38], three plant-derived lectins (*Wisteria floribunda* agglutinin, WFA; soybean agglutinin, SBA; and *Galanthus nivalis* agglutinin, GNA), characterized by different saccharide specificities, were compared. WFA has specificity for LacdiNAc ($\beta$-D-GalNAc-[1→4]-D-GlcNAc) sugars, with a lesser affinity for GalNac [39]. SBA binds to multiantennary carbohydrates with terminal GalNAc or Gal residues [40]. In contrast, GNA binds to sugars possessing high-mannose-type simple sugars [41]. The presence of WFA significantly enhanced EBOV PV entry. This effect was

observed in EBOV-GP variants and related GP proteins from other *Filovirus* species. WFA binding also reduced the neutralizing activity of an anti-GP monoclonal antibody (KZ52).

## METHODS

### Plasmids for virus GP expression

A codon-optimized sequence for the Makona isolate, Kissidougou-C15 GP (accession AHX24649.2), was synthesized and inserted into a pcDNA3.1 (Invitrogen). The generation of variant GP sequences from Makona C15 by *in vitro* mutagenesis was described in a previous study [42]. The plasmids encoding Ebola Mayinga GP and other *Ebolavirus* species were kind gifts from G. Kobinger (Galveston National Laboratory, University of Texas). Hepatitis C virus (HCV) H77 E1/E2 construct has been previously described [43]. The RABV (*Rabies lyssavirus*)-G protein construct was a kind gift of Dr E. Wright (University of Sussex), and the LCMV (*lymphocytic choriomeningitis mammarenavirus*)-G protein-encoding plasmid was generated in-house. The pM2D plasmid encoding the VSV (*Indiana vesiculovirus*)-G GP was obtained from AddGene (plasmid # 12259). The C15-ΔMLD construct was created by inverse PCR of the EBOV-C15 GP plasmid (primers available upon request) to generate a deletion of amino acids 305–485. Individual amino acid point mutants were generated using a Q5-SDM kit (NEB) using the B1 variant as the template.

### Production of pseudotype virus particles

Retroviral pseudotype viral particles (PVs) were produced as described previously [42]. In brief, $1.5\times10^6$ HEK-293T cells were seeded in a Primaria-coated 10 cm dish (Corning) and incubated overnight. Dishes were transfected with 2 µg of MLV-gag/pol encoding packaging plasmid phCMV-5349, 2 µg of the MLV-Luc plasmid pTG126 and 2 µg of plasmid encoding the viral envelope protein of interest. For the generation of EBOV-PVs, cells were transfected with 0.2 µg of plasmid encoding EBOV-GP. Negative control 'No GP' particles were generated by transfection without a viral envelope protein-encoding plasmid. For each transfection, plasmids were diluted in serum-free Opti-MEM (Gibco), mixed with 24 µl polyethylenimine (PEI) (Polysciences) in a final volume of 600 µl and incubated for 1 h at room temperature. Cell media was replaced with 7 ml Opti-MEM, and plasmid-PEI solution was added in a dropwise manner. Following a 6 h incubation at 37 °C, the Opti-MEM was replaced with 10 ml DMEM. Cell supernatants were harvested 72 h post-transfection and passed through a 0.2 µm syringe filter (Sartorius) and stored at 4 °C.

### Transduction assays

HuH7 cells [44] were used for the majority of transduction experiments. For specific transduction in NPC1-KO cells, previously described U2OS cell lines were used. These cells were seeded at a density of $1.5\times10^4$ cells per well in a 96-well white plate (Corning) and grown overnight. Media was aspirated from the wells and replaced with 100 µl of pseudotype virus (PV)-containing supernatant. For incubation with tetrameric lectins, WFA (Sigma L1516), SBA (Sigma L1395) or GNA (Sigma L8275) were diluted from a 10 mg $ml^{-1}$ stock solution to the required final concentration in the pseudotype-containing media. Incubation with lectins was performed for 1 h before infecting target cells. The inoculum was removed after 4 h, and 200 µl of DMEM was added per well, and cells were incubated for 72 h. When performing experiments adding lectins either before or after transduction, HuH7 target cells were washed four times with PBS (Sigma) before (or after) the addition of pseudotypes. To measure luciferase activity, media was removed, and cells were lysed in 50 µl cell lysis buffer (Promega) and incubated at room temperature for 30 min with gentle agitation. Plates were then read using a BMG Fluostar Omega plate reader, primed with luciferase substrate with gain set to 3600.

### Antibody neutralization assays

The KZ52 antibody was produced using a HEK-293 Freestyle expression system (Thermo Fisher Scientific). In brief, plasmids encoding the KZ52 heavy chain and light chain (pORIgHIB and pORIgLB [45], respectively) were mixed with PEI at a ratio of 1:3 and incubated at room temperature for 1 h. Cell density was adjusted to $1\times10^6$ cells $ml^{-1}$, and plasmid-PEI mix was added. Transfected cultures were incubated for 72 h, and media was harvested. KZ52 concentration was determined using an in-house IgG ELISA assay using an anti-light-chain antibody to capture the IgG and an anti-heavy-chain HRP-conjugated antibody for detection. KZ52 was incubated with EBOV PVs with or without WFA for 1 h at room temperature, and 100 µl was added per well to HuH7 cells. Cells were incubated with EBOV PVs for 4 h at 37 °C, and media was replaced with fresh DMEM. Cells were grown for 72 h, and transduction was measured using the previously described luciferase assay.

### ELISA binding assays

Pseudotypes were purified from transfected HEK-293T cell supernatants by ultracentrifugation at 107,000 ***g*** for 180 min through a 20% sucrose cushion. Pellets were resuspended and analysed by Western blot using an anti-MLV p30 antibody (Sigma). Following quantification, equal quantities of pseudotypes were used for ELISA, either directly coated to NUNC Maxisorp microtitre plates or by capturing on plates coated at 10 µg $ml^{-1}$ with WFA. Pseudotypes were then detected using mAb KZ52, either in the presence or absence of WFA, incubated concurrently. Detection of bound KZ52 was achieved using an anti-human IgG alkaline phosphatase-conjugated antibody (Sigma, A3187), followed by development with pNPP (Sigma, N1891) and reading at 405 nm.

### Statistics

Data were analysed using GraphPad Prism software (version 10.3.1). For determining the $IC_{50}$ values of KZ52, data were normalized to a no-antibody control group, and nonlinear regression was performed using the log(agonist) vs. response-variable slope (four-parameter model, with the bottom parameter constrained to a value of 0). Multiple comparisons were performed with a one-way ANOVA, using either Sidak's test or Dunnett's test to account for multiple comparisons where appropriate. Where only two datasets were compared, a Student's t-test was used.

### Structural modelling

For identifying *N*-linked glycan sites, the amino acid sequence of the EBOV C15 GP1 protein was modelled using I-TASSER (https://zhanggroup.org/I-TASSER/) using PDB structure 6VKM as a scaffold. Representation of the generated model was visualized in ChimeraX (https://www.cgl.ucsf.edu/chimerax/). Modelling of the oligomeric structure of the trimeric $GP_{1,2}$ in complex with mAb KZ52 (PDB 3CSY) and the tetrameric WFA (5KXB) proteins was performed with ChimeraX.

## RESULTS

### Disaccharide-specific lectins specifically enhance *Ebolavirus* infection

To investigate the consequences of the presence of plant-derived lectins during viral entry, a retroviral pseudotype entry model was employed, incorporating full-length authentic viral GPs (Fig. 1). Two reference strains of Zaire EBOV were initially assessed, the Makona C15 (EBOV-C15) and WT Mayinga 1976 (EBOV-May). These strains represent the initial variant that appeared in the 2014 epidemic, and the original isolate of EBOV. GPs representing two other *Ebolavirus* species, *Sudan ebolavirus* (SUDV) and *Reston ebolavirus* (RESTV), were also assessed. The GPs of Zaire EBOV, SUDV and RESTV share conserved *N*-linked glycan sites at $N^{40}$, $N^{204}$, $N^{238}$, $N^{259}$, $N^{270}$, $N^{298}$, $N^{563}$ and $N^{618}$ (Fig. S1, available in the online Supplementary Material). In addition, pseudotypes possessing viral GPs recovered from other viruses with class I fusion proteins (LCMV), class III fusion proteins (VSV, G protein

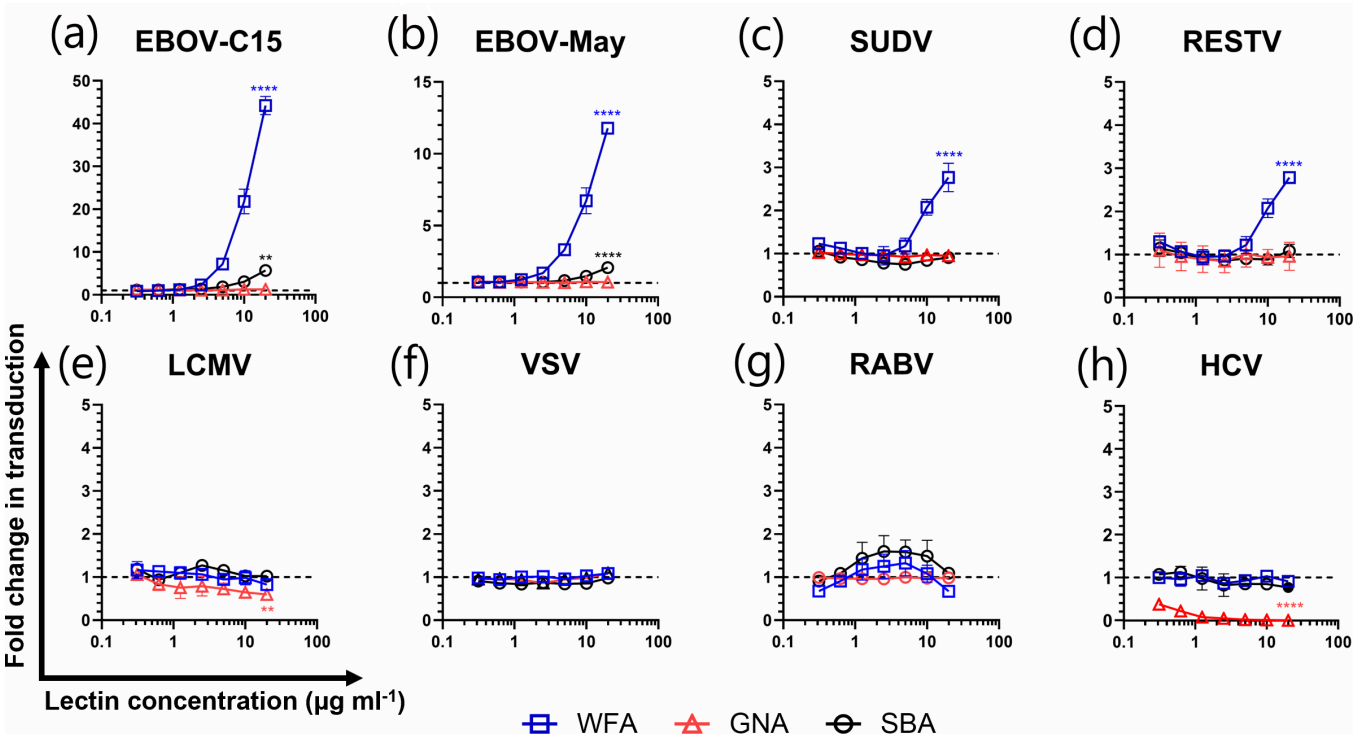


**Fig. 1.** Ebola virus GP-pseudotyped virus transduction is specifically enhanced in the presence of WFA. Pseudotyped virus particles possessing the envelope GPs of different viral species (including two strains of EBOV) were incubated with WFA, GNA or SBA prior to infection of human hepatoma (HuH7) cells. Each lectin was tested in a twofold dilution series in triplicate with a starting concentration of 20 µg $ml^{-1}$. Data are reported as fold change in transduction relative to a no-lectin control group. EBOV-C15, Makona EBOV; EBOV-May, Mayinga EBOV. The y-axis differs between graphs to aid visualization. Statistical significance between the effect observed at the highest concentration and a no-lectin control was determined by a one-way ANOVA followed by Dunnett's multiple comparison test, $^{**}P<0.01$ and $^{****}P<0.0001$. Data are from a single representative experiment. Each data point represents the mean of three technical repeats with errors displaying SD.

and RABV) and novel class fusion proteins (HCV E1/E2) [46] were included in this analysis. Each of these viral GPs exhibits *N*-linked glycosylation (SUDV-GP possesses 12 sites, RESTV-GP possesses 14, LCMV-GP possesses 11, both RABV-G and VSV-G possess 2 and HCV E1/E2 GPs together possess 16).

All pseudotypes were able to transduce HuH7 cells (Fig. S2A). Incubation of filovirus PVs with WFA prior to addition to target cells resulted in a dose-dependent increase in viral entry (Fig. 1a–d). At a WFA concentration of 20 μg ml$^{-1}$, the EBOV PVs displayed a significant mean fold increase of 44.2 ($P$<0.0001) and 11.8 ($P$<0.0001) for EBOV-C15 and EBOV-May, respectively (Fig. 1a, b). SUDV and RESTV also displayed enhanced viral entry when compared to a no-lectin control group (Fig. 1c, d). These PVs showed enhancement at a reduced level compared to the EBOV PVs, with a mean fold increase in transduction of 2.8 and 2.9, respectively. No change in entry was observed for any other virus in response to the presence of WFA (Fig. 1e–h).

Consistent with previous reports, GNA neutralized HCV PV entry [47, 48] at all concentrations tested (Fig. 1h). At a concentration of 20 μg ml$^{-1}$, GNA exhibited a 0.4-fold reduction in LCMV PV entry which was significant compared to a no-lectin control ($P$<0.01) (Fig. S2B). No significant effects of GNA were observed towards any other PVs in the panel. Following treatment with SBA lectin at a concentration of 20 μg ml$^{-1}$, HCV PVs displayed a mean 0.23-fold reduction in transduction ($P$<0.05; Fig. S2B) which contrasted to EBOV-C15 and EBOV-May PVs, showing fold increases of 4.7 and 1.1, respectively. The presence of SBA did not impact the entry of other PVs in the panel.

### Lectin enhancement is mediated by direct interaction with viral GPs

To define how WFA enhancement of EBOV entry occurs, EBOV PV entry assays were performed with HuH7 cells that were treated with lectins either before, during or after infection with pseudotypes, with thorough washing between steps (Fig. 2a, b). Enhancement of both EBOV-C15 and EBOV-May entry was only observed when cells were co-treated with both PVs and lectin (Fig. 2a, b). The mean fold increase in transduction was found to be statistically significant for both EBOV-C15 and EBOV-May when compared to the untreated control group ($P$<0.01 and $P$<0.001, respectively; Fig. 2a, b). To confirm that binding of WFA to EBOV pseudotypes occurred directly, a lectin-capture ELISA was performed in which pelleted PV samples were incubated on an ELISA plate coated with WFA and detected using the KZ52 antibody. WFA captured both EBOV-C15 and EBOV-May PV particles (Fig. 2c). The specificity of this interaction was demonstrated by performing the enhancement of entry experiment with EBOV-C15 PVs in the presence of increasing concentrations of saccharides (GalNAc, GlcNAc and mannose), which are specific ligands for different lectins. Enhancement was reduced as increasing concentrations of GalNAc were incubated with the WFA, with no effect observed when using either GlcNAc or mannose (Fig. 2d). No effect on transduction was observed with the highest concentration of saccharide alone (Fig. 2d). No effect of the sugars on the entry of VSV PVs was observed (Fig. S3).

### Enhancement of EBOV entry by WFA is species-independent but NPC1-dependent

To determine if the enhancing effect of WFA upon EBOV PV entry was specific to human cells, further entry assays were performed with the EBOV-permissive HypLu/45.1 cell line derived from foetal lung tissue from the bat species *Hypsignathus monstrosus* [49] (a potential reservoir of EBOV) [50]. In agreement with the observed effect of WFA on EBOV-C15 entry in HuH7 cells (Fig. 3a), entry of EBOV-C15 into HypLu/45.1 cells was enhanced by the presence of WFA, albeit with approximately half of the effect when tested at 10 μg ml$^{-1}$ (Fig. 3b). We also investigated whether WFA-mediated enhancement of EBOV PV entry was independent of the normal NPC1-dependent entry pathway. A previously validated NPC1 knockout U2OS cell line was utilized [7]. The enhancing effect of WFA on EBOV-C15 entry in U2OS cells was comparable to that observed for HuH7 cells (Fig. 3c). U2OS-NPC1 KO cells did not permit EBOV-C15 PV entry (Fig. 3d). WFA was unable to facilitate EBOV PV entry into these cells, demonstrating that the process supporting entry facilitated by WFA remained NPC1-dependent. Unexpectedly, for the control VSV PVs, the inclusion of WFA during infection was found to enhance infection when using U2OS-NPC1-KO cells as targets (Fig. 3d). This contrasted with all previous experiments conducted with both human and bat cell lines.

### WFA-mediated enhancement of EBOV entry is modulated by the presence of individual polymorphic *N*-linked glycosylation in the glycan cap

The Zaire EBOV-GP undergoes extensive glycosylation, with 17 *N*-linked glycan sites across the protein. To identify key glycosylation sites that mediate WFA enhancement of EBOV PV entry, transduction assays were performed using five previously described naturally occurring variants of the EBOV-C15 GP that lack *N*-linked glycosylation sites [42] (Fig. 4). These variants all possess an A82V mutation, located in the head region of $GP_1$, that became established early during the 2013–2016 EBOV epidemic [51] and is thought to enhance viral membrane fusion [52, 53]. This variant was labelled 'B1'. In addition, variant B12 encodes a T206M mutation, whilst variants B13, B14 and B16 each possess a T230A mutation, both of which disrupt *N*-linked glycosylation sequons, preventing glycosylation at residues $N^{228}$ and $N^{204}$, respectively (Table S1). The B1 variant was included as a control for the A82V mutation, as this variant was not predicted to have an altered *N*-linked glycosylation pattern compared to the EBOV-C15 control, and preliminary experiments showed that B1 PVs exhibited the same pattern of enhancement as EBOV-C15 (Fig. S4). In line with previous observations, each of the variant EBOV PVs exhibited enhanced entry in the presence of WFA (Fig. S5). When compared to a no-lectin control group, B1 and B12 showed a significant fold change of 23.8 ($P$<0.01)

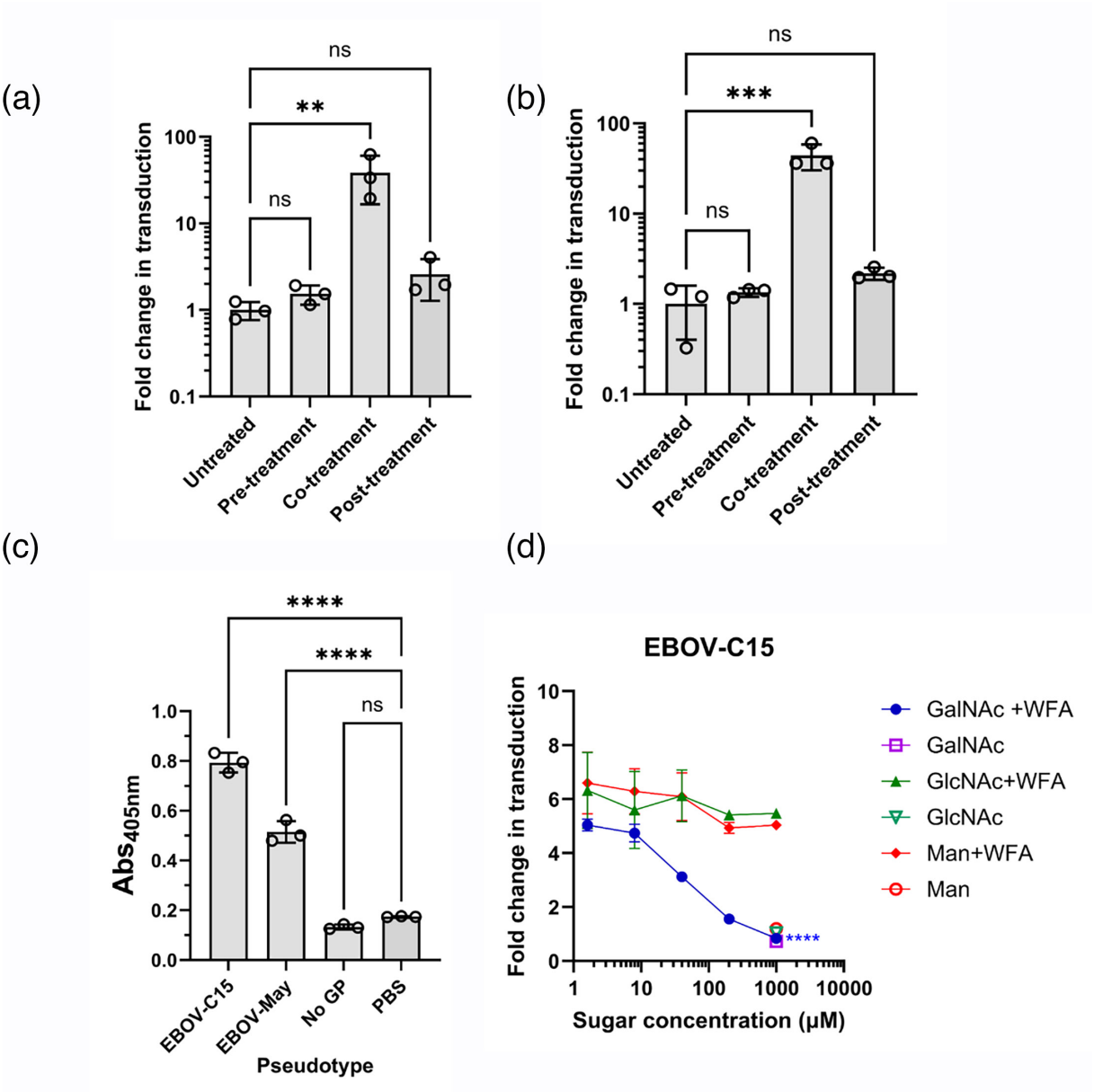


**Fig. 2.** Direct interaction of WFA and EBOV-GP results in enhancement. WFA was added at a final concentration of 10 µg ml$^{-1}$ to HuH7 cells at different stages of EBOV-C15 (a) and EBOV-May (b) PV entry. Cells were pre-treated with WFA prior to the addition of EBOV PVs. In the co-treatment condition, EBOV PVs and WFA were added simultaneously and incubated for 1 h. Post-treated WFA was added post-EBOV PV incubation. PV entry was measured by the luciferase reporter expression, and RLU values were compared with the untreated group. (c) The binding of pseudotypes to WFA was assessed by ELISA. Virus particles were incubated with coated WFA, and binding was revealed with incubation with anti-GP antibodies. Particles lacking GP were used as a negative control. (d) The specificity of interaction was determined by incubating GalNAc, GlcNAc or mannose with WFA during the co-treatment with EBOV-C15 pseudotype entry into HuH7 cells. Statistical significance was determined using one-way ANOVA followed by Dunnett's multiple comparison test, $P$<0.01 (**), $P$<0.001 (***), $P$<0.0001 (****) and $P$>0.05 (ns). Data are from a single representative experiment. Each data point represents the mean of three technical repeats with error bars displaying SD.

and 22.5 ($P$<0.01), respectively (Fig. 4a). Variants lacking glycosylation at residue N$^{228}$ – B13, B14 and B16 – exhibited lower levels of enhancement, with mean fold changes of 12.3 ($P$<0.01), 14.2 ($P$<0.05) and 14.5 ($P$<0.05), respectively (Figs 4a and S5). Surprisingly, each variant was also significantly enhanced by the SBA lectin at a concentration of 10 µg ml$^{-1}$, and GNA lectin did not impact EBOV or VSV PV entry (Fig. S5).

To quantify the effect of polymorphisms in the EBOV-GP$_1$, these five naturally occurring variants were analysed alongside three previously described *in vitro*-generated mutants [54] made in a B1 background, M1 (N238D), M2 (T270V) and M3 (T298V),

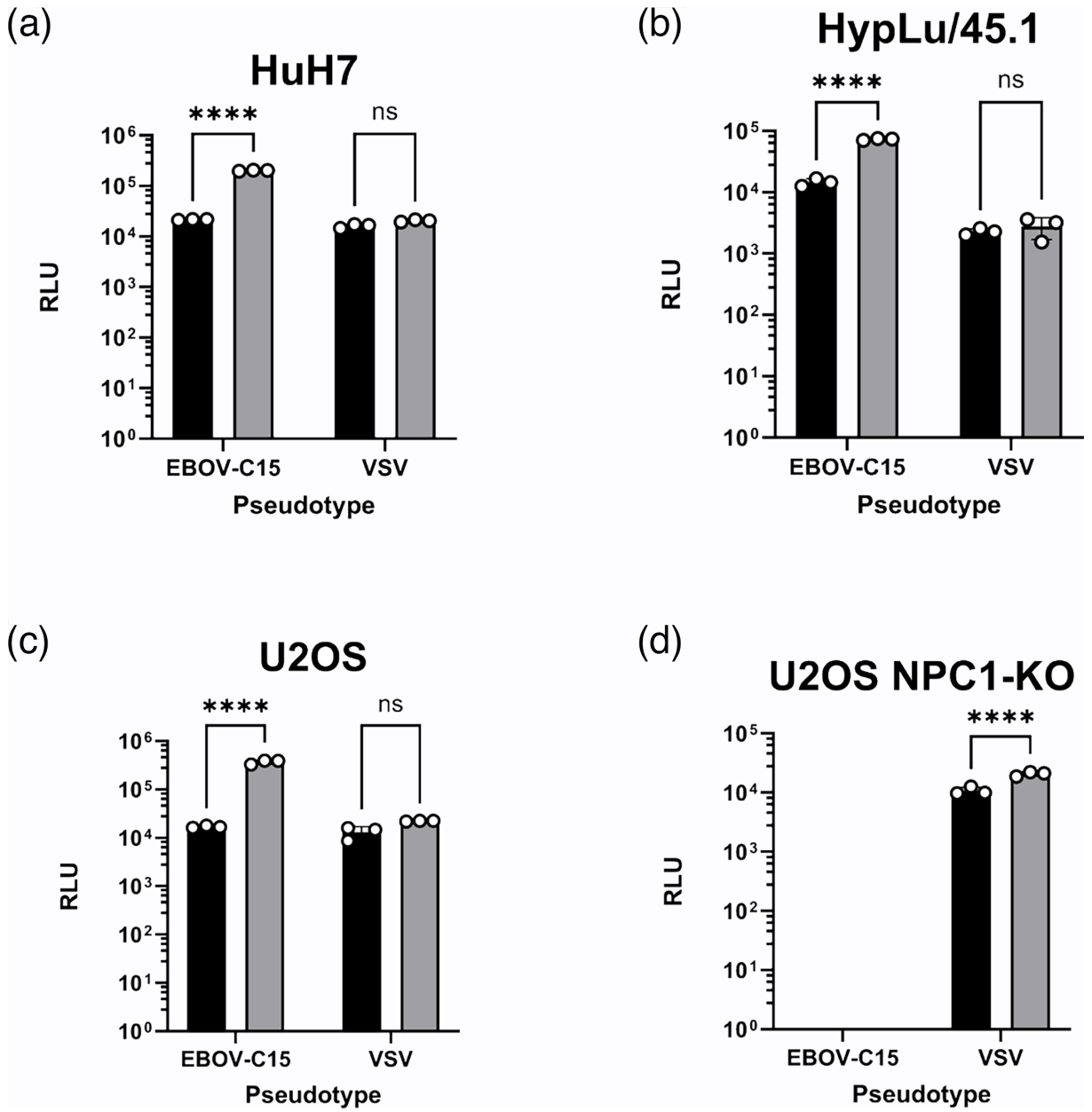


**Fig. 3.** WFA-mediated enhancement of entry occurs in different species and is NPC1-dependent. Four mammalian cell lines, HuH7 (human, a) and HpyLu/45.1 (bat, b), human osteosarcoma cells (U2OS, c) and a validated U2OS NPC1-knock-out cell line (d), were transduced with pseudotypes possessing the GPs of Ebola C15 or VSV, +/−WFA at a concentration of 10 µg ml$^{-1}$. Black bars indicate the control-treated pseudotypes, and grey bars indicate the WFA-treated pseudotypes. Significance was determined by one-way ANOVA followed by Sidak's multiple comparison test, ns $P$>0.05 and ****$P$<0.0001. Data are from a single representative experiment. Each data point represents the mean of three technical repeats with error bars displaying SD.

resulting in loss of glycosylation at $N^{238}$, $N^{268}$ and $N^{296}$, respectively. Normalizing for the differences in transduction observed for each mutant, enhancement was compared to the B1 reference (Fig. 4b). All pseudotypes possessing the T230A polymorphism had significantly reduced enhancement (B13, $P$<0.01; B14, $P$<0.05; B16, $P$<0.05), whilst entry enhancement of the T298V mutant was significantly increased ($P$<0.05) (Fig. 4b). When modelled on a structure of the $GP_1$ molecule based on PDB accession number 6VKM, the residues that impacted on WFA-mediated enhancement were found to be separated from those that did not (Fig. 4c). When visualized with the NPC1 binding pocket, the distance between the $N^{228}$ and the $I^{113}$ within the NPC1 binding site was measured to be ~18 Å.

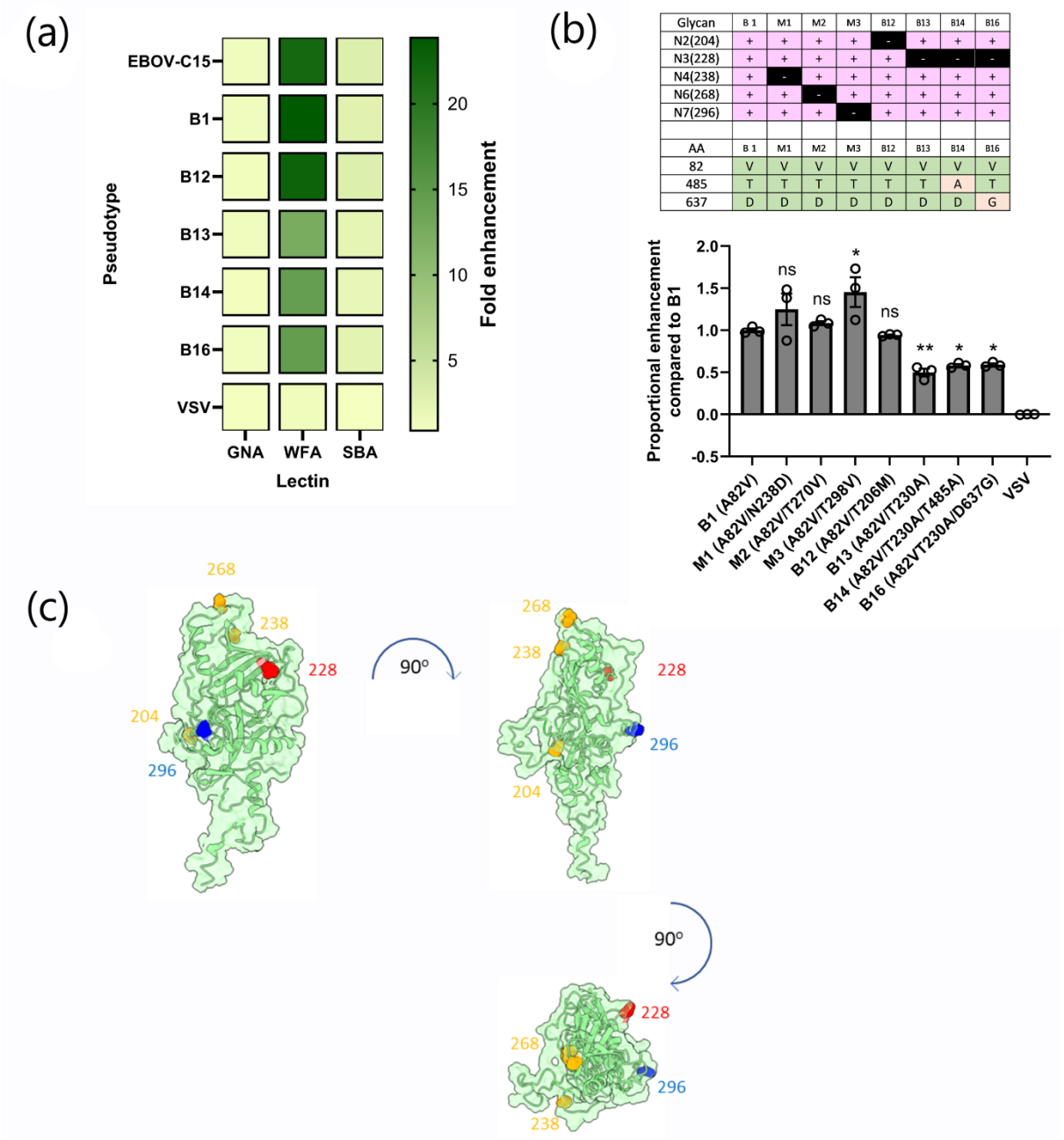


**Fig. 4.** WFA-mediated enhancement of entry is modified in naturally occurring *Ebolavirus* variants. (a) Infection assays using HuH7 cells were performed using GPs from naturally occurring EBOV isolates with predicted altered *N*-linked glycosylation sites from the WT C15. Fold change between each lectin was compared to a no-lectin control. (b) Three *in vitro*-generated glycan mutants, M1, M2 and M3, were compared with variants B1, B12, B13, B14 and B16 in the enhancement assay at 10 µg ml$^{-1}$. Differences were determined using one-way ANOVA and a Dunnett's multiple comparison test, ns $P$>0.05, *$P$<0.05 and **$P$<0.01. (c) Representation of the sites of *N*-linked glycosylation on a model of the Mayinga EBOV-GP$_1$ protein (produced using I-TASSER using the Makona C15 amino acid sequence modelled onto PDB structure 6VKM). Sites where removal of the glycan did not affect enhancement are highlighted in yellow, site (296) that increased enhancement is highlighted in blue and site (228) that reduced enhancement is highlighted in red.

In addition to individual amino acid variants, a modified clone of EBOV-C15 was generated possessing a complete MLD deletion (EBOV-C15-ΔMLD, removing aa305-485 of GP$_1$). This contained eight fewer *N*-linked glycosylation sites (Table S1) and removed the majority of *O*-linked glycosylation sites [13]. In line with previous reports [9], the EBOV-C15-ΔMLD mutant displayed a greater level of infectivity compared to the WT EBOV-C15 PVs (Fig. S6). Both EBOV-C15 and EBOV-C15-ΔMLD PVs were susceptible to enhancement by WFA lectin (Fig. 5a, b). Interestingly, at a WFA concentration of 10 µg ml$^{-1}$, the removal of the MLD significantly increased the enhancing effect of WFA from a mean fold change of 8.74–12.62 ($P$<0.0001; Fig. 5c). Additional

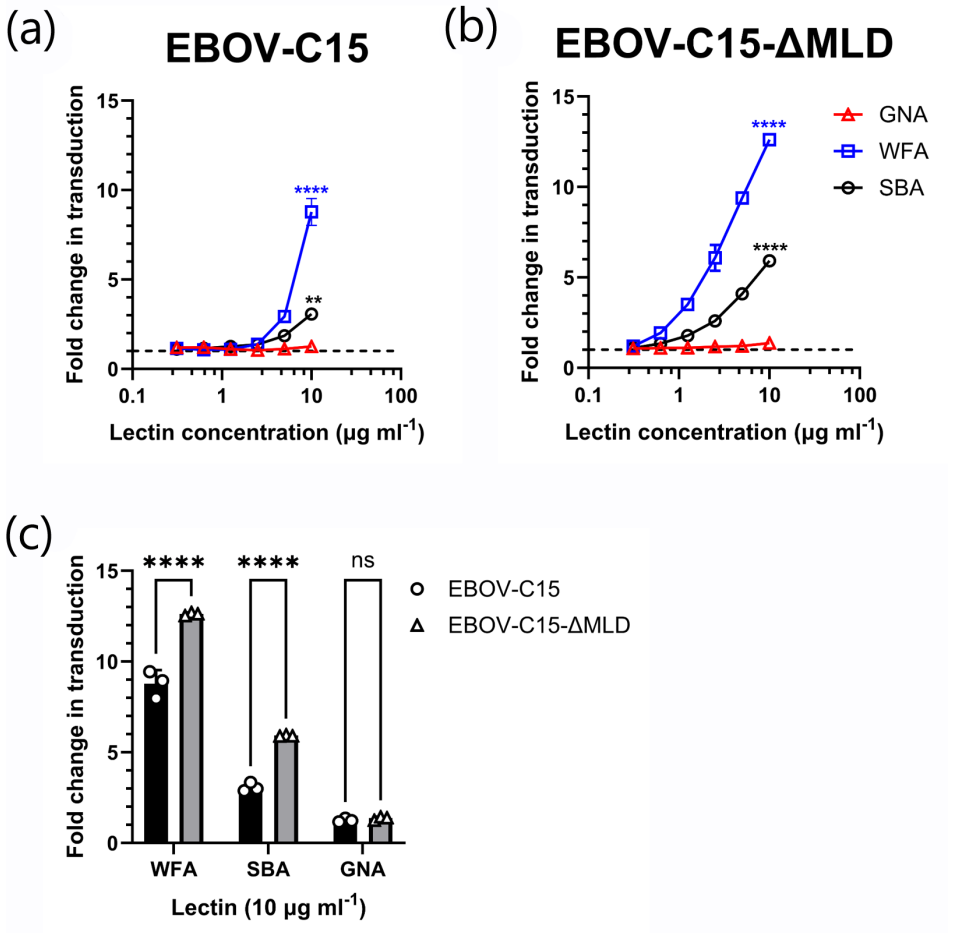


**Fig. 5.** Enhanced entry of mucin domain-deleted mutant of *Ebolavirus* C15 by WFA. Transduction assays with HuH7 cells were performed in triplicate with EBOV-C15 (a) and EBOV-C15-ΔMLD (b) PVs using twofold serially diluted lectins starting from 10 μg ml$^{-1}$. (c) Fold change in transduction of EBOV-C15 and EBOV-C15-ΔMLD at a lectin concentration of 10 μg ml$^{-1}$. Black bars indicate pseudotypes possessing the EBOV-C15 GP; grey bars indicate pseudotypes possessing the EBOV-C15-ΔMLD GP. Comparisons were determined by one-way ANOVA followed by Sidak's multiple comparison test, $P$>0.05 (ns) and $P$<0.0001 (****). Data are from a single representative experiment. Each data point represents the mean of three technical repeats with error bars displaying SD.

enhancement by SBA was also revealed in the absence of the MLD from a mean fold change in transductions of 3.07–5.92 ($P$<0.0001) (Fig. 5c).

### Reduced antibody-mediated neutralization of WFA-treated EBOV PVs

To determine if the binding of WFA to the EBOV-GP complex resulted in altered GP antigenicity, the impact of WFA on antibody-mediated neutralization and binding was investigated. Neutralization assays were performed with the well-characterized conformation-dependent anti-GP nAb, KZ52[6] against EBOV PVs in the presence of WFA. EBOV PVs bearing C15-GP or ΔMLD-GP were susceptible to neutralization by KZ52 in both the presence and absence of WFA (Fig. 6a). For EBOV-C15 PV, the $IC_{50}$ value of KZ52 was 5.85 μg ml$^{-1}$ in the presence of WFA and 3.86 μg ml$^{-1}$ without WFA (Fig. 6a and Table S2). The $IC_{50}$ values of KZ52 for ΔMLD-GP PV were 16.76 and 2.07 μg ml$^{-1}$ in the presence or absence of WFA, respectively (Fig. 6a and Table S2). To further confirm a potential KZ52 blocking effect by WFA, an ELISA was performed in which KZ52 binding to pelleted EBOV PVs was measured in the presence and absence of WFA (Fig. 6b). Binding of KZ52 to both EBOV-C15 and EBOV-C15-ΔMLD was partially reduced ($P$<0.001 and $P$<0.0001, respectively, Fig. 6b). Modelling of the interaction of WFA with contacts at the $N^{228}$ residue in the context of a trimeric presentation of the trimer of $GP_{1,2}$ heterodimers in complex with KZ52 Fabs (Fig. 6c) highlighted that, in the context of full $GP_{1,2}$, binding of WFA to the EBOV spike protein most likely occurs without directly blockading the KZ52 epitope. However, certain orientations of the tetrameric lectin could potentially compete with the antibody for binding.

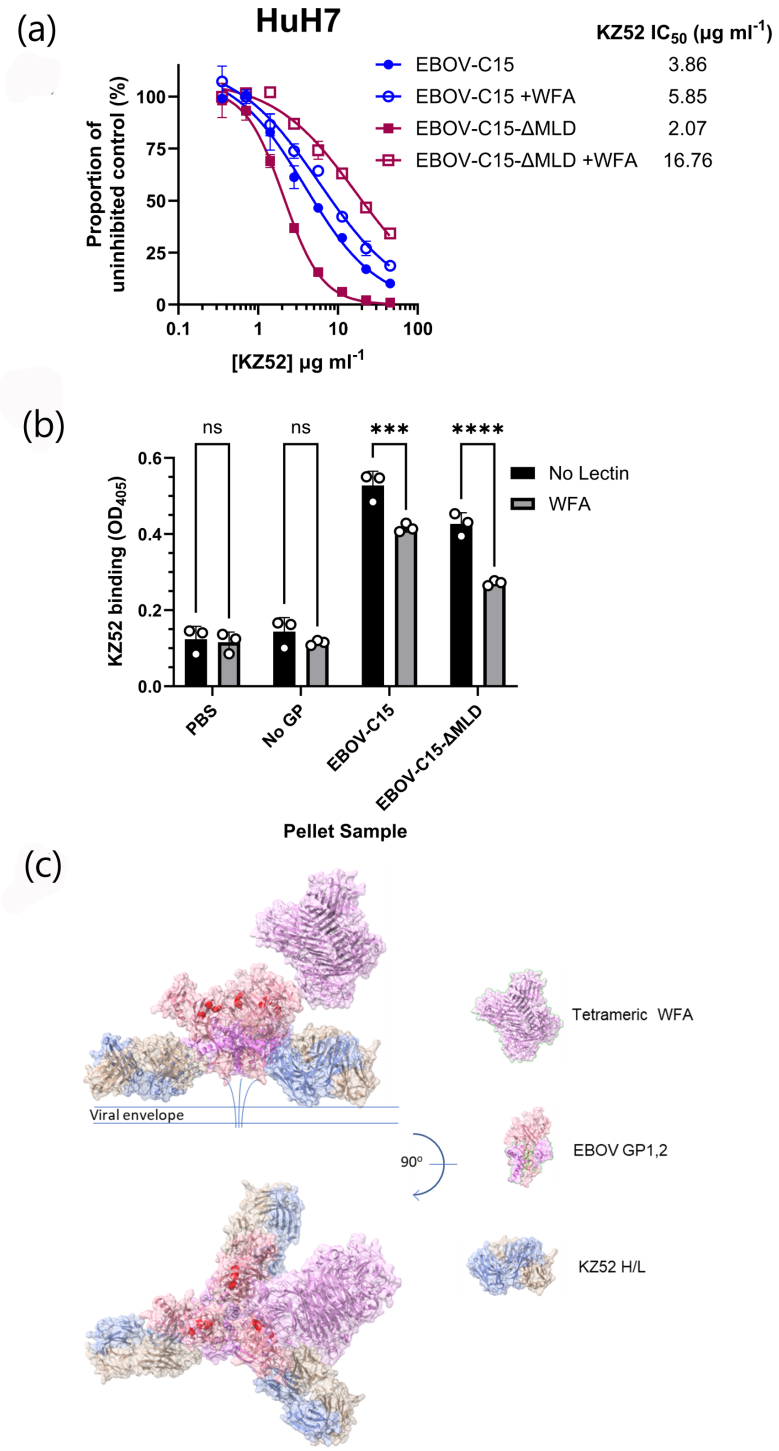


**Fig. 6.** Modelling of WFA binding to EBOV-GP. (a) mAb KZ52 neutralization of EBOV-C15 pseudotype entry into HuH7 cells in the presence or absence of WFA lectin. EBOV PVs possessing the C15 or C15-ΔMLD GPs were incubated with a twofold serial dilution of KZ52 in the absence or presence of WFA, at a final concentration of 10 µg ml$^{-1}$. Data were normalized to a no-antibody control, and each data point represents the mean of three technical repeats with error bars displaying SD. (b) Binding of KZ52 to EBOV PVs in a direct ELISA. Antibody was incubated with PVs in the presence or absence of WFA at 10 µg ml$^{-1}$. Significance was determined by one-way ANOVA followed by Sidak's multiple comparison test, ns $P$>0.05, ***$P$<0.001 and ****$P$<0.0001. Data are from a single representative experiment. Each data point represents the mean of three technical repeats with error bars displaying SD. (c) Modelling of the trimeric EBOV-GP in complex with KZ52 (PDB 3CSY) with one possible configuration of the tetrameric WFA molecule (PDB 5KXB) in close association with $N^{228}$ of $GP_1$ was performed using ChimeraX. Amino acid residues implicated in the NPC1 interaction are highlighted in red.

## DISCUSSION

This study provides the first evidence of plant-derived lectins enhancing EBOV-GP-mediated cell entry. Initial testing of three different plant lectins identified WFA as a potent enhancer of filovirus GP-mediated cellular entry. Two lectins were observed to enhance infection (WFA and SBA), but because the effect was most potent for WFA, this was investigated in more detail. However, the GalNAc- or Gal-specific SBA may exhibit similar properties to WFA. It remains to be determined why some plant lectins, such as mannose-specific BanLec[37], inhibit infection, but others have enhancing effects on filovirus entry. Of the filovirus species tested, EBOV displayed the greatest levels of enhancement in the presence of WFA, suggesting amino acid sequence-dependent activity. Enhancement was also observed in naturally occurring variants of the EBOV-GP that display altered patterns of *N*-linked glycosylation. Furthermore, greater WFA-mediated enhancement occurred following the deletion of the MLD region, which contrasts with the MLD-dependent enhancement previously described for human ficolin-1 [32]. Together, this indicates that the binding of WFA to EBOV-GP occurs at GalNAc-containing glycans present in the glycan cap of $GP_1$. The glycosylation of $GP_1$ is highly heterogeneous, with many complex glycans associated with each site. In human cells, each *N*-linked glycan site is predicted to possess, on average, 12 glycan compositions [13]. The data presented here support the conclusion that carbohydrate structures possessing accessible LacdiNAc or GalNAc are present on the surface of the $GP_1$ glycan cap. Given the restricted range of sugars attached to $N^{257}$ in $GP_1$[13], and the impact of variants observed here, it is most likely that these sugars are present at positions $N^{40}$ or $N^{228}$, or to *O*-linked sugars present in the glycan cap [55]. The confirmation that removing $N^{228}$ reduced but did not ablate enhancement confirms that this is a complex effect mediated by multiple glycans. Whilst $N^{40}$ is completely conserved across all filovirus species, $N^{228}$ is present in EBOV and RESTV, but not SUDV GP (Fig. S1). The reduction in enhancement observed for the $N^{228}$ mutant suggests that this residue contains a glycan presenting a ligand for WFA. The enhancement of infection for this variant was comparable to that of *Sudan ebolavirus* and *Reston ebolavirus*. Other sites contribute to the enhanced infection, and whilst direct protein-protein interactions cannot be excluded, it is likely that patterns of other conserved glycans contribute to the observed effect. Whilst we did not explore the effect of altering the potential *O*-linked glycosylation sites in this study, it is plausible that these contribute to the enhancing effect of WFA. GalNAc-containing *O*-linked sugars have been identified on the $GP_1$ by MS [55]. It is challenging to accurately predict the number of *O*-linked glycans attached to the $GP_{1,2}$ structure [55], but two *O*-linked sites in $GP_1$ have been well characterized [13]. Further investigations are required to determine the contribution of *O*-linked glycosylation to lectin-mediated entry enhancement.

The data presented in this study support a model of enhancement where the binding of WFA results in conformational changes to the GP complex that enhance receptor binding interactions. The demonstration that pre-treatment of cells with WFA before infection with EBOV pseudotypes does not enhance infection argues against a direct binding interaction between WFA and cellular factors. Enhancement of EBOV PV entry by WFA was also observed only when NPC1 was present. These observations suggest that late-stage entry pathways remain unchanged by WFA. The NPC1 receptor resides in endosomal membranes, and the formation of the GP-NPC1 complex requires cleavage of the glycan cap from the EBOV-GP. This stage is a prerequisite for the fusion of virus–host membranes. Thus, it is likely that WFA increases the rate of an earlier step in the entry process such as cellular attachment and/or internalization. Clear mechanisms for these stages of EBOV cellular entry remain to be identified. Although entry remained NPC1-dependent in the presence of WFA, it was observed that the level of enhancement was diminished in a bat cell line derived from *H. monstrosus*. This was possibly due to differing interactions between EBOV PV and host factors. NPC1 is highly conserved between these two species; however, the C domain involved in EBOV-GP binding differs by 23 amino acids [56], one of which resides in the binding interface with EBOV-GP [57]. To date, the structure of *H. monstrosus* NPC1 has not been resolved, thus limiting current understanding of how similar this protein is to the human analogue.

A potential limitation to this study was the reliance on a retroviral pseudoviral model of EBOV entry. This is a tractable approach to model entry of pathogenic viruses under containment level 2 laboratory settings. PVs have been used to model EBOV-GP function and processing and have the benefit of targeting the entry cascade alone. However, there are noted differences between EBOV PVs and the authentic virus. For example, EBOV PVs have been shown to be more resistant to the action of EBOV-neutralizing mAbs compared to the live virus [58, 59]. Alternative models for studying EBOV, such as virus-like particles [60] or VSV-based pseudotypes [58], could also be used for these studies, which may reproduce the morphology of the virus particles more accurately. However, the glycosylation of EBOV pseudotypes is similar to authentic GP [61], and these have been used previously to investigate the EBOV entry pathway [62]. The results presented here provide evidence that could be further explored with both a VLP infection assay and live virus cultures to confirm the observed enhancing effect in other models of EBOV entry. The choice of target cells for infection assays may also influence the outcome of experiments. In the present study, the HuH7 cell lines were utilized for the majority of experiments as they do not express DC-SIGN/L-SIGN, hMGL or LSECtin but do express high quantities of ASGPR1 [63, 64]. Our confirmation of the same enhancing effect in U2OS cells, which express much lower levels of ASGPR1, and non-human cells demonstrates that the enhancing effect is likely to be generalizable to all cell types. Further studies are required to assess the enhancing effect of WFA on cells expressing the complete range of membrane-associated lectins that may interact with the EBOV-GP.

Additionally, it is important for future work to investigate the impact of the WFA quaternary structure upon the enhancement. In nature, WFA exists in a tetrameric form allowing for the binding of four ligands per molecule. It would be of interest to test monomeric forms of WFA for enhancement of EBOV PVs. Whilst beyond the scope of the current study, this could be achieved through the identification of sites that are critical to tetramerization, followed by the characterization of specific point mutants that only form monomers.

The observation that WFA-treated EBOV PVs were less well neutralized by the KZ52 mAb indicated that WFA may either partially occlude the KZ52 epitope or that a change occurs upon WFA binding that alters the overall conformation of the GP complex, either to impact antibody binding or accelerate entry kinetics. KZ52 recognizes residues 505–514 and 549–556 of $GP_2$ and residues 42–43 of $GP_1$ [6]. Our modelling of the interaction of the WFA with glycosylation sites in GP demonstrated that binding to the oligomeric GP complex is possible without directly blockading the KZ52 binding site (Fig. 6c). It is plausible that conformational changes induced by lectin binding indirectly alter the epitope of this conformation-dependent antibody, and given that the $N^{228}$ residue is located at a site between the NPC1 binding site and the $GP_2$ subunit, but not directly overlapping, the blockade by WFA may not be direct. Further structural studies are required to resolve these possible interpretations of our data.

Collectively, the data presented here provide evidence that interactions between GalNAc-specific lectins and the EBOV-GP result in changes to the envelope GP that result in greater binding and fusion through an NPC1-dependent process. It is plausible that enhancement caused by lectins expressed in mammalian cells exhibits a similar mode of action. We propose a model of entry where initial, generalizable interactions with lectins (whether soluble or membrane-associated) trigger conformational changes that facilitate internalization and subsequent interaction with NPC1, negating the requirement for proposed lectin receptors [32] expressed on the surface of cells to mediate virus entry. This is consistent with previous assessments of the role of DC-SIGN in entry [28, 65]. The demonstration that the enhancing effect of WFA is more pronounced when using a ΔMLD construct highlights the possibility that lectin interactions may be promoted after the initial cell surface interactions and subsequent cathepsin B/L cleavage of $GP_1$ prior to NPC1 interaction.

Funding information
This work was funded by the Medical Research Council UK (grant MR/S009434/1).

Acknowledgements
We are grateful for the provision of glycoprotein-expression constructs from the laboratories of Edward Wright and Gary Kobinger. We are also grateful to Kartik Chandran and colleagues for the provision of the U2OS NPC1-knockout cell line. We would also like to acknowledge the contribution of undergraduate research project students who contributed to preliminary experiments for this study.

Conflicts of interest
The authors declare that there are no conflicts of interest.

References

1. Letafati A, Salahi Ardekani O, Karami H, Soleimani M. Ebola virus disease: a narrative review. *Microb Pathog* 2023;181:106213.
2. Feldmann H, Geisbert TW. Ebola haemorrhagic fever. *Lancet* 2011;377:849–862.
3. Aruna A, Mbala P, Minikulu L, Mukadi D, Bulemfu D, *et al*. Ebola virus disease outbreak - Democratic Republic of the Congo, August 2018-November 2019. *MMWR Morb Mortal Wkly Rep* 2019;68:1162–1165.
4. Kyobe Bosa H, Kamara N, Aragaw M, Wayengera M, Talisuna A, *et al*. The West Africa Ebola virus disease outbreak: 10 years on. *Lancet Glob Heal* 2024;12:e1081–e1083.
5. Feldmann H, Volchkov VE, Volchkova VA, Ströher U, Klenk H-D. Biosynthesis and role of filoviral glycoproteins. *J Gen Virol* 2001;82:2839–2848.
6. Lee JE, Fusco ML, Hessell AJ, Oswald WB, Burton DR, *et al*. Structure of the Ebola virus glycoprotein bound to an antibody from a human survivor. *Nature* 2008;454:177–182.
7. Spence JS, Krause TB, Mittler E, Jangra RK, Chandran K. Direct visualization of Ebola virus fusion triggering in the endocytic pathway. *mBio* 2016;7:e01857-15.
8. Nathan L, Lai AL, Millet JK, Straus MR, Freed JH, *et al*. Calcium ions directly interact with the Ebola virus fusion peptide to promote structure-function changes that enhance infection. *ACS Infect Dis* 2020;6:250–260.
9. Chandran K, Sullivan NJ, Felbor U, Whelan SP, Cunningham JM. Endosomal proteolysis of the Ebola virus glycoprotein is necessary for infection. *Science* 2005;308:1643–1645.
10. Carette JE, Raaben M, Wong AC, Herbert AS, Obernosterer G, *et al*. Ebola virus entry requires the cholesterol transporter Niemann-Pick C1. *Nature* 2011;477:340–343.
11. Bornholdt ZA, Ndungo E, Fusco ML, Bale S, Flyak AI, *et al*. Host-primed Ebola virus GP exposes a hydrophobic NPC1 receptor-binding pocket, revealing a target for broadly neutralizing antibodies. *mBio* 2016;7:e02154–15.
12. Iraqi M, Edri A, Greenshpan Y, Kundu K, Bolel P, *et al*. N-glycans mediate the Ebola virus-GP1 shielding of ligands to immune receptors and immune evasion. *Front Cell Infect Microbiol* 2020;10:48.
13. Peng W, Rayaprolu V, Parvate AD, Pronker MF, Hui S, *et al*. Glycan shield of the ebolavirus envelope glycoprotein GP. *Commun Biol* 2022;5:785.
14. Takada A, Robison C, Goto H, Sanchez A, Murti KG, *et al*. A system for functional analysis of Ebola virus glycoprotein. *Proc Natl Acad Sci USA* 1997;94:14764–14769.
15. Alvarez CP, Lasala F, Carrillo J, Muñiz O, Corbí AL, *et al*. C-type lectins DC-SIGN and L-SIGN mediate cellular entry by Ebola virus in cis and in trans. *J Virol* 2002;76:6841–6844.
16. Simmons G, Reeves JD, Grogan CC, Vandenberghe LH, Baribaud F, *et al*. DC-SIGN and DC-SIGNR bind ebola glycoproteins and enhance infection of macrophages and endothelial cells. *Virology* 2003;305:115–123.

17. Lepenies B, Lang R. Editorial: lectins and their ligands in shaping immune responses. *Front Immunol* 2019;10:2379.
18. Mason CP, Tarr AW. Human lectins and their roles in viral infections. *Molecules* 2015;20:2229–2271.
19. Zhang W, Bouwman KM, van Beurden SJ, Ordonez SR, van Eijk M, *et al*. Chicken mannose binding lectin has antiviral activity towards infectious bronchitis virus. *Virology* 2017;509:252–259.
20. Verma A, White M, Vathipadiekal V, Tripathi S, Mbianda J, *et al*. Human H-ficolin inhibits replication of seasonal and pandemic influenza A viruses. *J Immunol* 2012;189:2478–2487.
21. Avirutnan P, Hauhart RE, Marovich MA, Garred P, Atkinson JP, *et al*. Complement-mediated neutralization of dengue virus requires mannose-binding lectin. *mBio* 2011;2:1–11.
22. Jalal PJ, Urbanowicz RA, Horncastle E, Pathak M, Goddard C, *et al*. Expression of human ficolin-2 in hepatocytes confers resistance to infection by diverse hepatotropic viruses. *J Med Microbiol* 2019;68:642–648.
23. Brown KS, Keogh MJ, Owsianka AM, Adair R, Patel AH, *et al*. Specific interaction of hepatitis C virus glycoproteins with mannan binding lectin inhibits virus entry. *Protein Cell* 2010;1:664–674.
24. Hamed MR, Brown RJP, Zothner C, Urbanowicz RA, Mason CP, *et al*. Recombinant human L-ficolin directly neutralizes hepatitis C virus entry. *J Innate Immun* 2014;6:676–684.
25. Lin G, Simmons G, Pöhlmann S, Baribaud F, Ni H, *et al*. Differential N-linked glycosylation of human immunodeficiency virus and Ebola virus envelope glycoproteins modulates interactions with DC-SIGN and DC-SIGNR. *J Virol* 2003;77:1337–1346.
26. Takada A, Fujioka K, Tsuiji M, Morikawa A, Higashi N, *et al*. Human macrophage C-type lectin specific for galactose and N-acetylgalactosamine promotes filovirus entry. *J Virol* 2004;78:2943–2947.
27. Messingham KN, Richards PT, Fleck A, Patel RA, Djurkovic M, *et al*. Multiple cell types support productive infection and dynamic translocation of infectious Ebola virus to the surface of human skin. *Sci Adv* 2025;11:eadr6140.
28. Marzi A, Möller P, Hanna SL, Harrer T, Eisemann J, *et al*. Analysis of the interaction of Ebola virus glycoprotein with DC-SIGN (dendritic cell-specific intercellular adhesion molecule 3-grabbing nonintegrin) and its homologue DC-SIGNR. *J Infect Dis* 2007;196 Suppl 2:S237–46.
29. Ji X, Olinger GG, Aris S, Chen Y, Gewurz H, *et al*. Mannose-binding lectin binds to Ebola and Marburg envelope glycoproteins, resulting in blocking of virus interaction with DC-SIGN and complement-mediated virus neutralization. *J Gen Virol* 2005;86:2535–2542.
30. Michelow IC, Lear C, Scully C, Prugar LI, Longley CB, *et al*. High-dose mannose-binding lectin therapy for Ebola virus infection. *J Infect Dis* 2011;203:175–179.
31. Brudner M, Karpel M, Lear C, Chen L, Yantosca LM, *et al*. Lectin-dependent enhancement of Ebola virus infection via soluble and transmembrane C-type lectin receptors. *PLoS One* 2013;8:e60838.
32. Favier A-L, Gout E, Reynard O, Ferraris O, Kleman J-P, *et al*. Enhancement of Ebola virus infection via ficolin-1 interaction with the mucin domain of GP glycoprotein. *J Virol* 2016;90:5256–5269.
33. Tsaneva M, Van Damme EJM. 130 years of plant lectin research. *Glycoconj J* 2020;37:533–551.
34. Mazalovska M, Kouokam JC. Lectins as promising therapeutics for the prevention and treatment of HIV and other potential coinfections. *Biomed Res Int* 2018;2018:3750646.
35. Marchetti M, Mastromarino P, Rieti S, Seganti L, Orsi N. Inhibition of herpes simplex, rabies and rubella viruses by lectins with different specificities. *Res Virol* 1995;146:211–215.
36. Swanson MD, Boudreaux DM, Salmon L, Chugh J, Winter HC, *et al*. Engineering a therapeutic lectin by uncoupling mitogenicity from antiviral activity. *Cell* 2015;163:746–758.
37. Covés-Datson EM, Dyall J, DeWald LE, King SR, Dube D, *et al*. Inhibition of Ebola virus by a molecularly engineered banana lectin. *PLoS Negl Trop Dis* 2019;13:e0007595.
38. Sanchez A, Yang ZY, Xu L, Nabel GJ, Crews T, *et al*. Biochemical analysis of the secreted and virion glycoproteins of Ebola virus. *J Virol* 1998;72:6442–6447.
39. Haji-Ghassemi O, Gilbert M, Spence J, Schur MJ, Parker MJ, *et al*. Molecular basis for recognition of the cancer glycobiomarker, LacdiNAc (GalNAc[$\beta$1→4]GlcNAc), by Wisteria floribunda Agglutinin. *J Biol Chem* 2016;291:24085–24095.
40. Gupta D, Bhattacharyya L, Fant J, *et al*. Observation of unique cross-linked lattices between multiantennary carbohydrates and soybean lectin. presence of pseudo-2-fold axes of symmetry in complex type carbohydrates. *Biochemistry* 1994;33.
41. Shibuya N, Goldstein IJ, Van Damme EJ, Peumans WJ. Binding properties of a mannose-specific lectin from the snowdrop (*Galanthus nivalis*) bulb. *J Biol Chem* 1988;263:728–734.
42. Urbanowicz RA, McClure CP, Sakuntabhai A, Sall AA, Kobinger G, *et al*. Human adaptation of Ebola virus during the West African outbreak. *Cell* 2016;167:1079–1087.
43. Urbanowicz RA, McClure CP, King B, Mason CP, Ball JK, *et al*. Novel functional hepatitis C virus glycoprotein isolates identified using an optimized viral pseudotype entry assay. *J Gen Virol* 2016;97:2265–2279.
44. Nakabayashi H, Taketa K, Miyano K, Yamane T, Sato J. Growth of human hepatoma cells lines with differentiated functions in chemically defined medium. *Cancer Res* 1982;42:3858–3863.
45. Metheringham RL, Pudney VA, Gunn B, Towey M, Spendlove I, *et al*. Antibodies designed as effective cancer vaccines. *MAbs* 2009;1:71–85.
46. Augestad EH, Holmboe Olesen C, Grønberg C, Soerensen A, Velázquez-Moctezuma R, *et al*. The hepatitis C virus envelope protein complex is a dimer of heterodimers. *Nature* 2024;633:704–709.
47. Shaw J, Gosain R, Kalita MM, Foster TL, Kankanala J, *et al*. Rationally derived inhibitors of hepatitis C virus (HCV) p7 channel activity reveal prospect for bimodal antiviral therapy. *elife* 2020;9:1–36.
48. Ashfaq UA, Masoud MS, Khaliq S, Nawaz Z, Riazuddin S. Inhibition of hepatitis C virus 3a genotype entry through Glanthus Nivalis Agglutinin. *Virol J* 2011;8:248.
49. Kühl A, Hoffmann M, Müller MA, Munster VJ, Gnirss K, *et al*. Comparative analysis of Ebola virus glycoprotein interactions with human and bat cells. *J Infect Dis* 2011;204 Suppl 3:S840–9.
50. Leroy EM, Kumulungui B, Pourrut X, Rouquet P, Hassanin A, *et al*. Fruit bats as reservoirs of Ebola virus. *Nature* 2005;438:575–576.
51. Diehl WE, Lin AE, Grubaugh ND, Carvalho LM, Kim K, *et al*. Ebola virus glycoprotein with increased infectivity dominated the 2013–2016 epidemic. *Cell* 2016;167:1088–1098.
52. Wang MK, Lim SY, Lee SM, Cunningham JM. Biochemical basis for increased activity of Ebola glycoprotein in the 2013–16 epidemic. *Cell Host Microbe* 2017;21:367–375.
53. Fels JM, Bortz RH 3rd, Alkutkar T, Mittler E, Jangra RK, *et al*. A glycoprotein mutation that emerged during the 2013–2016 Ebola virus epidemic alters proteolysis and accelerates membrane fusion. *mBio* 2021;12:03616–03620.
54. Lennemann NJ, Rhein BA, Ndungo E, Chandran K, Qiu X, *et al*. Comprehensive functional analysis of N-linked glycans on Ebola virus GP1. *mBio* 2014;5:e00862-13.
55. Collar AL, Clarke EC, Anaya E, Merrill D, Yarborough S, *et al*. Comparison of N- and O-linked glycosylation patterns of ebolavirus glycoproteins. *Virology* 2017;502:39–47.
56. Ng M, Ndungo E, Kaczmarek ME, Herbert AS, Binger T, *et al*. Filovirus receptor NPC1 contributes to species-specific patterns of ebolavirus susceptibility in bats. *elife* 2015;4:1–22.
57. Wang H, Shi Y, Song J, Qi J, Lu G, *et al*. Ebola viral glycoprotein bound to its endosomal receptor Niemann-Pick C1. *Cell* 2016;164:258–268.
58. Steeds K, Hall Y, Slack GS, Longet S, Strecker T, *et al*. Pseudotyping of VSV with Ebola virus glycoprotein is superior to HIV-1 for the assessment of neutralising antibodies. *Sci Rep* 2020;10:14289.
59. Cantoni D, Wilkie C, Bentley EM, Mayora-Neto M, Wright E, *et al*. Correlation between pseudotyped virus and authentic virus

neutralisation assays, a systematic review and meta-analysis of the literature. *Front Immunol* 2023;14:1184362.

60. Watanabe S, Watanabe T, Noda T, Takada A, Feldmann H, *et al*. Production of novel ebola virus-like particles from cDNAs: an alternative to ebola virus generation by reverse genetics. *J Virol* 2004;78:999–1005.
61. Wang B, Wang Y, Frabutt DA, Zhang X, Yao X, *et al*. Mechanistic understanding of N-glycosylation in Ebola virus glycoprotein maturation and function. *J Biol Chem* 2017;292:5860–5870.
62. Jeffers SA, Sanders DA, Sanchez A. Covalent modifications of the ebola virus glycoprotein. *J Virol* 2002;76:12463–12472.
63. Uhlén M, Fagerberg L, Hallström BM, Lindskog C, Oksvold P, *et al*. Tissue-based map of the human proteome. *Science* 2015;347:1260419.
64. Jin H, Zhang C, Zwahlen M, von Feilitzen K, Karlsson M, *et al*. Systematic transcriptional analysis of human cell lines for gene expression landscape and tumor representation. *Nat Commun* 2023;14:5417.
65. Matsuno K, Nakayama E, Noyori O, Marzi A, Ebihara H, *et al*. C-type lectins do not act as functional receptors for filovirus entry into cells. *Biochem Biophys Res Commun* 2010;403:144–148.